OXFORD

Cerebral Cortex, 2023, **33**, 5501–5506
https://doi.org/10.1093/cercor/bhac437
Advance access publication date 12 January 23
Original Article

Quantitative morphometric changes in vascular mild cognitive impairment patients: early diagnosis of dementia

Jitian Guan[1,†], Qiuyu Li[1,†], Zhuozhi Dai[1,†], Lingfeng Lai[1,†], Shuyi Sun[1,†], Yiqun Geng[2], Zhiwei Shen[1], Lan Luo[1], Yanlong Jia[1], Lin Yang[1], Yanyan Tang[1], Gen Yan[3,*], Renhua Wu[1,*]

[1]Department of Radiology, The 2nd Affiliated Hospital, Medical College of Shantou University, Shantou 515041, China,
[2]Laboratory of Molecular Pathology, Shantou University Medical College, Shantou 515041, China,
[3]Department of Radiology, The Second Affiliated Hospital of Xiamen Medical College, Xiamen 515041, China

*Corresponding authors: Department of Radiology, The Second Affiliated Hospital of Xiamen Medical College, Xiamen, China. Email: gyan@stu.edu.cn (Gen Yan); Department of Radiology, The Second Affiliated Hospital of Shantou University Medical College, Shantou, China. Email: cjr.wurenhua@vip.163.com (Renhua Wu)

†Jitian Guan, Qiuyu Li, Zhuozhi Dai, Lingfeng Lai and Shuyi Sun are the co-first author.

Vascular mild cognitive impairment (VMCI) is an early and reversible stage of dementia. Volume differences in regional gray matter may reveal the development and prognosis of VMCI. This study selected 2 of the most common types of VMCI, namely, periventricular white matter hyperintensities (PWMH, $n = 14$) and strategic single infarctions (SSI, $n = 10$), and used the voxel-based morphometry method to quantify their morphological characteristics. Meanwhile, age- and sex-matched healthy volunteers were included ($n = 16$). All the participants were neuropsychologically tested to characterize their cognitive function and underwent whole-brain magnetic resonance imaging scanning. Our results showed that the volumes of the bilateral temporal lobes and bilateral frontal gray matter were obviously diminished in the PWMH group. The atrophy volume difference was 4,086 voxels in the left temporal lobe, 4,154 voxels in the right temporal lobe, 1,718 voxels in the left frontal lobe, and 1,141 voxels in the right frontal lobe ($P \leq 0.001$). Moreover, the characteristics of the gray matter atrophy associated with the PWMH were more similar to those associated with Alzheimer's disease than SSI, which further revealed the susceptibility for escalation from PWMH to dementia. In conclusion, PWMH patients and SSI patients have different morphological characteristics, which explain the different prognoses of VMCI.

Key words: magnetic resonance imaging; voxel-based morphometry; vascular mild cognitive impairment; temporal lobe; atrophy.

Introduction

Vascular cognitive impairment is a mental disorder caused by or related to vascular diseases (Dichgans and Leys 2017; Iadecola et al. 2019), ranging from its mildest form, vascular mild cognitive impairment (VMCI), to complete dementia syndrome. VMCI is a condition in which the impairment affects ≥1 cognitive domains but is not severe enough to guarantee a diagnosis of dementia, which is one of the early signs of dementia. Since VMCI is reversible under appropriate treatment, early diagnosis is particularly important (Frances et al. 2016). Moreover, different types of VMCI have diverse prognoses. Previous statistical studies have indicated that, compared to other types of VMCI, mild cognitive impairment associated with periventricular white matter hyperintensities (PWMH) more easily deteriorates into dementia (Park et al. 2016; Rutten-Jacobs et al. 2017). However, the mechanism underlying this effect is unclear.

PWMH is a radiological condition characterized by lesions around the lateral ventricles, which is associated with microinfarction (Liu et al. 2016). Another common and widely studied type of VMCI is caused by strategic single infarctions (SSI), such as infarctions in the thalamus or caudate head (Weaver et al. 2021). However, previous studies indicated that, in rare cases, a single strategic lesion might result in serious and widespread cognitive impairment, leading to a diagnosis of dementia (Zheng et al. 2016). The different prognoses between these two types of VMCI patients need to be explored further.

Atrophy is an essential indicator of secondary degeneration after cerebral infarction. Meta-analyses have shown that general cerebral atrophy is associated with the development of cognitive impairment after vascular disorders (Wang et al. 2021). In addition, cortical gray matter atrophy is an independent predictor of cognitive decline in patients with subcortical cerebrovascular injury, and the severity of dementia is associated with cortical gray matter atrophy (Trapp et al. 2018).

Compared with other traditional volume assessment methods, voxel-based morphometry (VBM) provides an automated, voxel-wise comparison of structure volumes between different patient subsets (Zhang et al. 2016; Keller et al. 2018). This process involves normalizing all magnetic resonance imaging (MRI) scan objects into a common anatomical space to eliminate the differences in brain size and shape between individuals. In this spatial normalization process, images are normalized to standard templates (image databases based on normalized stereotaxic atlases) or custom templates explicitly created for the study through linear and nonlinear transformations. The images of each subject were then automatically segmented into gray matter, white matter, and

Received: August 31, 2022. **Revised:** October 8, 2022. **Accepted:** October 9, 2022

cerebrospinal fluid regions and were smoothed using a Gaussian filter (Torres et al. 2016; Kan et al. 2020).

We assumed regional volume differences between patients with PWMH and SSI suffering from mild cognitive impairment, which account for the diverse prognoses. In the present study, we compared the regional differences between patients with PWMH and those with SSI, and a sample of ischemic patients without cognitive impairment was also recruited. In addition, VBM was used to adjust individual brain distortions to a common template (Guo et al. 2019). We sought to determine the effectiveness of this approach in classifying gray matter changes in VMCI and further understand the relationship between gray matter changes and cognitive function.

Materials and methods

Participants

All the experimental protocols were approved by the Ethics Committee of Shantou University Medical College. A total of 24 outpatients or inpatients with cerebral infarction were enrolled in our neurology department, including 15 males and 9 females, with an average age of 69 ± 3.2 years. The diagnosis was made according to Erkinjutti's criteria (Erkinjuntti et al. 2000): (i) Clinical criteria: (1) symptoms and signs of paroxysmal mild upper motor neuron damage; (2) abnormal gait, instability, and easy to fall in the early stage; (3) early urinary control is poor; (4) Bulbar paralysis and extrapyramidal signs; (5) highlight the executive function and attention; and (6) depression, personality, and behavior abnormalities. (ii) MRI criteria: (1) white matter damage type: extensive deep and ventricular voiceover lesions, lacunar infarcts with extended cap longer than 10 mm (measured along the anterior ventricular angular axis) or irregular halos (>10 mm in width, irregular edges, extending into deep white matter) and/or diffuse fused hyperintensity (>25 mm, irregular) or extensive white matter lesions (diffuse hyperintensity without boundaries) and deep gray matter; (2) lacunar protrusion type: at least 5 lacunar foci in deep gray matter; (3) no cortical or subcortical nonlacunar artery innervation area infarction, watershed infarction, hemorrhage, normal intracranial pressure hydrocephalus, or other particular etiological white matter lesions.

Exclusion criteria: (i) complicated with cortical infarction; massive cerebral infarction; (ii) poor general condition, or combined with aphasia or lateral limb paralysis, unable to cooperate with cognitive function measurement; (iii) cognitive impairment or dementia caused by causes other than the cerebrovascular disease (such as tumor, epilepsy, psychosis, hypothyroidism, liver and kidney insufficiency, alcohol or drug abuse); and (iv) patients with cognitive dysfunction before infarction.

Sixteen healthy volunteers with an average age of 57.9 ± 6.5 years were selected as the standard control group. The control and 2 patient groups were matched in gender and age. All subjects signed informed consent.

Neuropsychological assessment

All the patients underwent neuropsychological testing, including assessments for attention, language abilities, praxis, the 4 elements of Gerstmann syndrome, visuoconstructive functioning, verbal, and visual memory, and frontal/executive functioning. The scorable tests included the following: the Montreal cognitive assessment (MoCA), activities of daily living (ADL), Clinical Dementia Rating Scale (CDR), and Hamilton Depression Rating Scale (HDRS). The MCI criteria were as follows: $21 \leq \text{MoCA} \leq 26$, CDR = 0.5, ADL < 16, and HDRS < 8.

Acquisition of MR images

All the MRI scans were acquired using a 1.5-Tesla MRI scanner at the Second Affiliated Hospital of Shantou University Medical College. A high-resolution 3D spoiled gradient-recalled T_1-weighted MRI scan was acquired for each subject using the following identical imaging parameters: axial slices with a thickness of 1.4 mm, an echo time of 5 ms, a repetition time of 11.1 ms, the number of excitations at 1, a flip angle of 20°, a field of view of 240 × 240 mm, a matrix size of 256 × 256 pixels, NEX = 1, and 96 axial slices.

VBM image preprocessing

The imaging data were analyzed using the SPM8 software (Institute of Neurology, London, UK), implemented in MATLAB (Mathworks Inc., Sherborn, MA, United States). First, normalize each scan into a template, the Montreal Neurological Institute space. Adjusting the parameters through the "Estimate and Write" module, the individual 3D, T1-spoiled gradient-recalled scans were segmented into white matter, gray matter, and cerebrospinal fluid components. The individual gray matter segments were spatially normalized to the gray matter template. The quality of split and standardization was checked using the "Display One slice for all images" and "Check sample homovariance using covariance" options on the menu. During the normalization, the voxel sizes were multiplied by the Jacobian determinants, which were derived from the normalization process. The region segmented, normalized, and modulated individual brain segments were smoothed with an 8-mm full-width at half-maximum Gaussian kernel. By applying the smoothing kernel, interindividual variability was compensated, and the data were conformed more closely to the Gaussian random field theory, which provides the revised statistical inference.

Statistical analyses

The demographic, stroke-related variables, and the cognitive performance domain scores of the group differences were assessed using a 2-sample *t*-test where appropriate: SSI versus PWMH, SSI versus control group, and PWMH versus control group. The normalized, modulated, segmented, and smoothed lesion-adjusted MRI images were used to evaluate the gray matter differences among the 3 groups, respectively. The general linear model, controlling for the total brain volume and selected stroke-related, cognitive, and demographic variables were used to perform the voxel-by-voxel comparisons. A threshold of $P \leq 0.001$ indicated significant differences in the gray matter tissue volumes between the groups. Moreover, the clusters of significant differences required an extent of at least 50 voxels.

Results

Forty participants were recruited according to the medical images and neuropsychological tests, including 14 PWMH patients, 10 SSI patients, and 16 age- and sex-matched control group. There were no significant differences in the gender, age, or handedness distribution among these three groups. Compared to the SSI and control groups, the patients in the PWMH group had fewer years of formal education. However, the scores from the MoCA, ADL, CDR and HDRS assessments were all not significantly different.

The whole cerebral volume declined in the PWMH patients compared to the SSI and control groups. The regions of the gray matter volumes were derived from the VBM processing. The statistically significant differences between the PWMH and SSI groups are shown in Table 1. The most obvious atrophy was

Table 1. Stereotactic locations of the significant differences ($P \leq 0.001$ with a 50-voxel extent threshold) in the gray matter volumes between the SSI and PWMH groups.

	Talairach coordinates					
Location	X	Y	Z	k	Z	p
right superior temporal gyrus	51	−10	4	4154	5.59	0.001
left superior temporal gyrus	−57	−18	12	4086	5.34	0.001
left inferior frontal gyrus	−32	30	−9	1718	4.40	0.001
right lingual gyrus	23	−73	24	256	4.22	0.001
right middle frontal gyrus	3	29	−14	707	4.18	0.001
right inferior frontal gyrus	51	27	−9	434	4.04	0.001
primary visual cortex	12	−60	9	180	3.70	0.001
right cuneus	3	−84	3	118	3.51	0.001

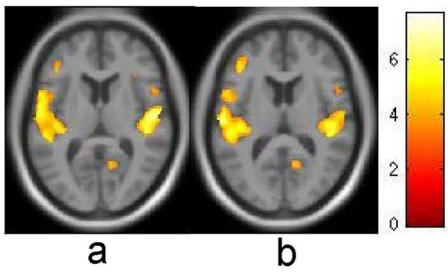

Fig. 1. Statistical maps of the gray matter volumes in the PWMH (a) and SSI (b) groups. Relative to the SSI group, the PWMH patients showed significant gray matter volume decreases in widespread regions of the bilateral temporal lobes. Additional regions of decreased gray matter volume in the PWMH group were found in the bilateral superior frontal lobes, left postcentral gyrus, bilateral inferior frontal gyrus, right middle frontal gyrus, and right lingual gyrus.

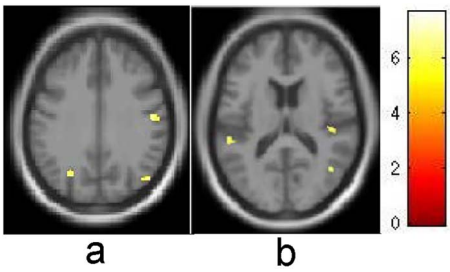

Fig. 2. Statistical maps of the gray matter volumes in the SSI (a) and control groups (b). The atrophy in the SSI patients was much more moderate. There were only several trivial atrophies in the postcentral gyrus, superior temporal gyrus, and occipital lobe.

observed in the superior temporal gyrus, with the regions in the left and right consisting of 4,086 voxels and 4,154 voxels, respectively ($P \leq 0.001$). The atrophy in both of the frontal lobes was also significant, involving 4,154 voxels in the left and 434 voxels in the right frontal lobe ($P \leq 0.001$). In addition, there were some slight decreases in the right lingual gyrus and cuneus.

Figure 1 depicts the statistical maps of the gray matter volumes in the most significant slices of the PWMH and SSI groups. Relative to the SSI group, the PWMH patients showed serious gray matter volume decreases in widespread regions of the bilateral temporal lobes. Additional regions of decreased gray matter volume were found in the bilateral superior frontal lobes, left postcentral gyrus, bilateral inferior frontal gyrus, right middle frontal gyrus, and right lingual gyrus.

The atrophy observed in the SSI patients was much more moderate. Although several gyri indicated significant differences, including the precentral gyrus, superior temporal gyrus, postcentral gyrus, occipital lobe, etc., the maximum voxel cluster was <300 (Table 2). Statistically significant atrophy was noted in the right temporal lobe and right postcentral gyrus in the SSI group compared with the control group (Fig. 2).

Inspection of the volume changes between the PWMH patients and healthy volunteers revealed dramatic atrophy in extensive gray matter regions, including the bilateral temporal lobes, postcentral gyrus, middle frontal gyrus, lingual gyrus, etc. (Fig. 3).

Table 2. Stereotactic Locations of Significant Differences ($P \leq 0.001$ with a 50-voxel extent threshold) in Gray Matter Volume between SSI and Control Group.

	Talairach Coordinate					
Location	X	Y	Z	K	Z	p
right precentral gyrus	36	−9	46	93	3.89	0.001
right superior temporal gyrus	48	−54	−21	211	3.81	0.001
left occipital lobe	−30	−67	34	73	3.76	0.001
right postcentral gyrus	51	−16	33	281	3.75	0.001
left postcentral gyrus	−38	−34	43	69	3.66	0.001
right middle temporal gyrus	44	−61	10	71	3.65	0.001
right postcentral gyrus	39	−28	46	194	3.51	0.001
left superior temporal gyrus	−54	−37	15	68	3.45	0.001
right thalamus	15	−30	0	54	3.31	0.001

Table 3. Stereotactic locations of the significant differences ($P \leq 0.001$ with a 50-voxel extent threshold) in the gray matter volumes between the PWMH and control groups.

	Talairach Coordinates					
Location	X	Y	Z	K	Z	p
left superior temporal gyrus	−57	−4	6	13,112	6.09	0.001
right superior temporal gyrus	48	−27	15	10,668	5.46	0.001
right middle frontal gyrus	26	33	34	869	4.98	0.001
left middle temporal gyrus	−59	−33	−3	2037	4.39	0.001
right lingual gyrus	14	−58	10	507	4.24	0.001
right cuneus	23	−73	25	617	4.20	0.001

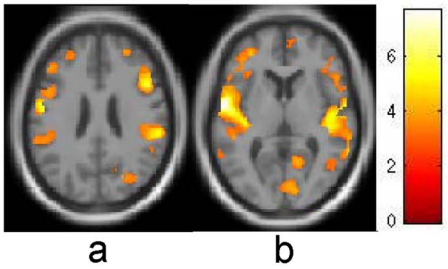

Fig. 3. Statistical maps of the gray matter volumes in the PWMH (a) and control groups (b). Decreased gray matter volumes were detected in the PWMH group compared with the control group in the bilateral temporal lobes, right postcentral gyrus, right middle frontal gyrus, and right lingual gyrus. The scope of the decrement was more extensive.

The atrophy volume in the superior temporal gyrus reached ~10,000 voxels (Table 3).

Discussion

By analyzing baseline imaging data, we demonstrated that compared with age-matched control participants, VMCI patients had reduced brain volume, which was most pronounced in the bilateral temporal lobes. In a previous longitudinal follow-up study, patients with lacunar stroke and leukoaraiosis had twice the atrophy rate of age-matched control participants, which was approximately 1% per year (Appleton et al. 2020). By contrast, no cognitive changes were detected during this period. The sensitivity of brain volume measurements over time suggests that they may have potential as surrogate markers for detecting the disease progression and assessing the efficacy.

In previous studies, volume changes were also compared between patients with SSI with and without cognitive impairment. Significant decreases were found in the thalamus in patients with ischemic stroke and cognitive impairment (Kim et al. 2020). However, limited data have suggested that patients with SSI identify as a high-risk group, and the rate of progression to dementia is slow (Graff-Radford et al. 2020). Recent studies provided evidence that extensive white-matter damage, such as PWMH, showed a stronger correlation with dementia compared with SSI.

The reason underlying PWMH being more closely related to cognitive decline than SSI is intriguing. Periventricular white matter contains several bundles that connect various parts of the brain, particularly in the brain cap region (Porcu et al. 2020). The periventricular cap region radiates through the inferior and superior occipito-frontal tracts, inferior longitudinal tract, cingulate gyrus, and thalamus; however, the density of these bundles are located in the deep white matter region (Tan et al. 2019). This suggests that the significant association of PWMH with cortical thinning and executive dysfunction may be related to the major regions crossing these regions. In addition, bundles passing through the anterior cap interconnect the frontal lobe structure primarily with other structures. Specifically, anterior thalamic radiation connects the anterior thalamus to the orbitofrontal or dorsolateral frontal region.

The mechanism of brain atrophy in VMCI remains to be elucidated. Pathological and physiological variables that may affect brain volume have been investigated in the context of multiple sclerosis (Moccia et al. 2018). Factors contributing to reduced brain volume may be related to axonal loss, resolution of inflammation and edema, gliosis, demyelination, dehydration, normal aging, and antiinflammatory agents (Andravizou et al. 2019; Arvanitakis et al. 2019; Yang, Rong, et al. 2021). However, few studies have performed direct pathological investigations to analyze the histology underlying brain volume changes in VMCI (Yang, Wan, et al. 2021). Changes in brain volume may be a direct result of microvascular disease.

Atrophy of temporal lobe structures is a common indicator in patients with Alzheimer's disease, and it is associated with deficient performance in memory tests (Bregman et al. 2020; Caillaud et al. 2020). In our study, the atrophy of the temporal lobes was more marked in the patients with PWMH compared to that noted in those in the SSI and control groups. The characteristics of the gray matter atrophy associated with the PWMH were more similar to those associated with Alzheimer's disease than SSI, which may further reveal the susceptibility for escalation from PWMH to dementia. It is our hope that further exploration will eventually allow us to identify the early stages of dementia.

Traditional MRI measurement methods are based on the region of interest (ROI), which has certain defects, such as time consumption, intense subjectivity, poor repeatability, and inability to perform whole-brain analysis. However, using VBM to measure the morphological characteristics of PWMH and SSI can directly analyze the original data. There is no prior assumption on ROI, and it is not subject to the subjective influence of researchers, so it has the advantages of comprehensiveness, automaticity, objectivity, and repeatability.

However, in this study, after segmentation, standardization, and smoothing, the data of the 2 experimental groups were superimposed on the standardized brain map of a patient with cognitive impairment, which was more reasonable than superimposed on the SPM template. It can be further improved

in the future. Therefore, it is necessary to establish specific standard templates suitable for specific study populations in the future.

Conclusion

PWMH and SSI have different characteristics of gray matter atrophy, which explains the different clinical courses of PWMH and SSI from the morphology perspective. In addition, the similar features of gray matter atrophy between PWMH and neurodegenerative diseases suggest that this subtype of vascular cognitive impairment may be combined with or secondary to neurodegenerative diseases.

Acknowledgements

JG, QL, ZD, Lingfeng Lai (LL), and SS contributed equally to this work, including to the whole study conception and design, acquisition of data, and drafting of the manuscript. LL, SS, YG, ZS, LL, and YJ helped with the acquisition of data. LY, YT, and LL helped with the data processing. RW GY were the corresponding authors. All the authors reviewed the manuscript.

Funding

This work was supported by grants from the National Science Foundation of China (grant no. 31870981 and 82020108016), the 2020 LKSF Cross-Disciplinary Research (grant no. 2020LKSFBME06), the 2020 Li Ka Shing Foundation Cross-Disciplinary Research (grant no. 2020LKSFG05D), and the Grant for Key Disciplinary Project of Clinical Medicine under the Guangdong High-Level University Development Program (grant no. 002-18120302). Guangdong science and technology special Foundation (2021)88-27.

Conflict of interest statement: The authors declare that they have no known competing financial interests or personal relationships that could have appeared to influence the work reported in this paper.

References

Andravizou A, Dardiotis E, Artemiadis A, Sokratous M, Siokas V, Tsouris Z, Aloizou AM, Nikolaidis I, Bakirtzis C, Tsivgoulis G et al. Brain atrophy in multiple sclerosis: mechanisms, clinical relevance and treatment options. *Auto Immun Highlights*. 2019:10(1):7.

Appleton JP, Woodhouse LJ, Adami A et al. Imaging markers of small vessel disease and brain frailty, and outcomes in acute stroke. *Neurology*. 2020:94(5):e439–e452.

Arvanitakis Z, Shah RC, Bennett DA. Diagnosis and management of dementia: review. *JAMA*. 2019:322(16):1589–1599.

Bregman N, Kavé G, Zeltzer E, Biran I, Alzheimer's Disease Neuroimaging Initiative. Memory impairment and Alzheimer's disease pathology in individuals with MCI who underestimate or overestimate their decline. *Int J Geriatr Psychiatry*. 2020:35:581–588.

Caillaud M, Hudon C, Boller B, Brambati S, Duchesne S, Lorrain D, Gagnon JF, Maltezos S, Mellah S, Phillips N et al. Evidence of a relation between hippocampal volume, white matter hyperintensities, and cognition in subjective cognitive decline and mild cognitive impairment. *J Gerontol B Psychol Sci Soc Sci*. 2020:75(7):1382–1392.

Dichgans M, Leys D. Vascular cognitive impairment. *Circ Res*. 2017:120:573–591.

Erkinjuntti T, Inzitari D, Pantoni L, Wallin A, Scheltens P, Rockwood K, Roman GC, Chui H, Desmond DW. Research criteria for subcortical vascular dementia in clinical trials. *J Neural Transm Suppl*. 2000:59:23–30.

Frances A, Sandra O, Lucy U. Vascular cognitive impairment, a cardiovascular complication. *World J Psychiatry*. 2016:6:199–207.

Graff-Radford J, Aakre JA, Knopman DS, Schwarz CG, Flemming KD, Rabinstein AA, Gunter JL, Ward CP, Zuk SM, Spychalla AJ et al. Prevalence and heterogeneity of cerebrovascular disease imaging lesions. *Mayo Clin Proc*. 2020:95(6):1195–1205.

Guo J, Yang M, Biswal BB, Yang P, Liao W, Chen H. Abnormal functional connectivity density in post-stroke aphasia. *Brain Topogr*. 2019:32:271–282.

Iadecola C, Duering M, Hachinski V, Joutel A, Pendlebury ST, Schneider JA, Dichgans M. Vascular cognitive impairment and dementia: JACC scientific expert panel. *J Am Coll Cardiol*. 2019:73(25):3326–3344.

Kan H, Uchida Y, Arai N, Ueki Y, Aoki T, Kasai H, Kunitomo H, Hirose Y, Matsukawa N, Shibamoto Y. Simultaneous voxel-based magnetic susceptibility and morphometry analysis using magnetization-prepared spoiled turbo multiple gradient echo. *NMR Biomed*. 2020:33(5):e4272.

Keller SS, Roberts N, Baker G, Sluming V, Cezayirli E, Mayes A, Eldridge P, Marson AG, Wieshmann UC. A voxel-based asymmetry study of the relationship between hemispheric asymmetry and language dominance in Wada tested patients. *Hum Brain Mapp*. 2018:39(7):3032–3045.

Kim SJ, Lee DK, Jang YK, Jang H, Kim SE, Cho SH, Kim JP, Jung YH, Kim EJ, Na DL et al. The effects of longitudinal white matter hyperintensity change on cognitive decline and cortical thinning over three years. *J Clin Med*. 2020:9(8):E2663.

Liu Z, Zhao Y, Zhang H, Chai Q, Cui Y, Diao Y, Xiu J, Sun X, Jiang G. Excessive variability in systolic blood pressure that is self-measured at home exacerbates the progression of brain white matter lesions and cognitive impairment in the oldest old. *Hypertens Res*. 2016:39(4):245–253.

Moccia M, de Stefano N, Barkhof F. Imaging outcome measures for progressive multiple sclerosis trials. published correction appears in. *Mult Scler*. 2018:23:1614–1626 2017.

Park JH, Myung W, Choi J, Kim S, Chung JW, Kang HS, Na DL, Kim SY, Lee JH, Han SH et al. Extrapyramidal signs and cognitive subdomains in Alzheimer disease. *Am J Geriatr Psychiatry*. 2016:24(7):566–574.

Porcu M, Operamolla A, Scapin E, Garofalo P, Destro F, Caneglias A, Suri JS, Falini A, Defazio G, Marrosu F et al. Effects of white matter hyperintensities on brain connectivity and hippocampal volume in healthy subjects according to their localization. *Brain Connect*. 2020:10(8):436–447.

Rutten-Jacobs LCA, Markus HS, UK Young Lacunar Stroke DNA Study. Vascular risk factor profiles differ between magnetic resonance imaging-defined subtypes of younger-onset lacunar stroke. *Stroke*. 2017:48:2405–2411.

Tan SYZ, Keong NCH, Selvan RMP, Li H, Ooi LQR, Tan EK, Chan LL. Periventricular white matter abnormalities on diffusion tensor imaging of postural instability gait disorder parkinsonism. *AJNR Am J Neuroradiol*. 2019:40(4):609–613.

Torres US, Duran FL, Schaufelberger MS, Crippa JAS, Louzã MR, Sallet PC, Kanegusuku CYO, Elkis H, Gattaz WF, Bassitt DP et al. Patterns of regional gray matter loss at different stages of schizophrenia: a multisite, cross-sectional VBM study in first-episode and chronic illness. *NeuroImage Clin*. 2016:12:1–15.

Trapp BD, Vignos M, Dudman J, Chang A, Fisher E, Staugaitis SM, Battapady H, Mork S, Ontaneda D, Jones SE et al. Cortical

neuronal densities and cerebral white matter demyelination in multiple sclerosis: a retrospective study. *Lancet Neurol*. 2018: 17(10):870–884.

Wang F, Hua S, Zhang Y, Yu H, Zhang Z, Zhu J, Liu R, Jiang Z. Association between small vessel disease markers, medial temporal lobe atrophy and cognitive impairment after stroke: a systematic review and meta-analysis. *J Stroke Cerebrovasc Dis*. 2021:30(1):105460.

Weaver NA, Kuijf HJ, Aben HP, Abrigo J, Bae HJ, Barbay M, Best JG, Bordet R, Chappell FM, Chen CPLH et al. Strategic infarct locations for post-stroke cognitive impairment: a pooled analysis of individual patient data from 12 acute ischaemic stroke cohorts. *The Lancet Neurology*. 2021:20(6): 448–459.

Yang Z, Rong Y, Cao Z, Wu Y, Zhao X, Xie Q, Luo M, Liu Y. Microstructural and cerebral blood flow abnormalities in subjective cognitive decline plus: Diffusional Kurtosis Imaging and Three-Dimensional Arterial Spin Labeling Study. *Front Aging Neurosci*. 2021:13:625843.

Yang Z, Wan X, Zhao X, Rong Y, Wu Y, Cao Z, Xie Q, Luo M, Liu Y. Brain neurometabolites differences in individuals with subjective cognitive decline plus: a quantitative single- and multi-voxel proton magnetic resonance spectroscopy study. *Quant Imaging Med Surg*. 2021:11(9):4074–4096.

Zhang Z, Wang Y, Shen Z, Yang Z, Li L, Chen D, Yan G, Cheng X, Shen Y, Tang X et al. The neurochemical and microstructural changes in the brain of systemic lupus erythematosus patients: a multimodal MRI study. *Sci Rep*. 2016:6(1):19026.

Zheng L, Vinters HV, Mack WJ, Weiner MW, Chui HC, IVD Program Project. Differential effects of ischemic vascular disease and Alzheimer's disease on brain atrophy and cognition. *J Cereb Blood Flow Metab*. 2016:36(1):204–215.